

Heat Transfer Simulation in Solid Substrate Fermentation

G. Saucedo-Castañeda*, M. Gutiérrez-Rojas, G. Bacquet, M. Raimbault*, and G. Viniegra-González

Universidad Autónoma Metropolitana Iztapalapa, Depto. Biotecnología, AP 55-535, CP 09340, México D.F., México

Accepted for publication October 31, 1989

A mathematical model was developed and tested to simulate the generation and transfer of heat in solid substrate fermentation (SSF). The experimental studies were realized in a 1-L static bioreactor packed with cassava wet meal and inoculated with *Aspergillus niger*. A simplified pseudohomogeneous monodimensional dynamic model was used for the energy balance. Kinetic equations taking into account biomass formation (logistic), sugar consumption (with maintenance), and carbon dioxide formation were used. Model verification was achieved by comparison of calculated and experimental temperatures. Heat transfer was evaluated by the estimation of Biot and Peclet heat dimensionless numbers 5-10 and 2550-2750, respectively. It was shown that conduction through the fermentation fixed bed was the main heat transfer resistance. This model intends to reach a better understanding of transport phenomena in SSF, a fact which could be used to evaluate various alternatives for temperature control of SSF, i.e., changing air flow rates and increasing water content. Dimensionless numbers could be used as scale-up criteria of large fermentors, since in those ratios are described the operating conditions, geometry, and size of the bioreactor. It could lead to improved solid reactor systems. The model can be used as a basis for automatic control of SSF for the production of valuable metabolites in static fermentors.

INTRODUCTION

Solid substrate fermentation (SSF) advantages and disadvantages have been largely discussed.¹⁻³ Thermal characteristics of organic material and the low moisture content in SSF create specially difficult conditions for heat transfer. Although SSF is an alternative to the more conventional liquid fermentation,² it has been seen that temperature control in large scale solid fermentors is a difficult problem³ since conventional techniques and concepts used in submerged cultures are not easy to apply to SSF. Due to the nature of SSF, it seems interesting to apply concepts normally used in chemical catalytic reactors to study the mechanisms of heat transport.

Presented at the Eighth International Biotechnology Symposium, Paris, July 17-22, 1988.

* Current address: ORSTOM, Laboratoire de Biotecnologie, 2051, Av. du Val de Montferrand, BP 5045, 34032 Montpellier, FRANCE.

A large quantity of metabolic heat³ is produced during SSF, up to 3200 kcal/kg dry matter (DM) in composting systems⁴ and a temperature gradient of 3°C/cm in tempeh fermentation.⁵ Heat generation is directly related to the metabolic activities of the microorganisms, particularly respiration during growth, which is related to oxygen consumption and CO₂ formation.

In SSF of cassava by *Aspergillus niger*,⁶ nearly 35% of consumed sugars are oxidized by respiratory metabolism, producing approximately 80 kcal/h kg DM. The heat generated must be dissipated since microbial growth is very sensitive to a rise in temperature, affecting spore germination, growth, product formation, and sporulation. Different methods have been used to remove heat from the fermenting media.³

In fact, the use of stirred solid substrate fermentors can reduce system heterogeneity in comparison to static bed fermentation, and the macrogradients of a static bed could be decreased. However, the abrasion encountered in rotating systems can disrupt mold development. That is, in certain cases the use of static SSF reactors could be required by using forced-air currents as a cooling mean.⁷ In such cases, it is important to know the contributions of conduction and convection in the overall heat transfer mechanism.

Simulation of SSF in fixed packed bed bioreactors is an important feature in reactor design and control. Nevertheless, modeling is scanty in the literature.³ The presence of solids as well as the heterogeneity of the media have prevented the accurate determination of important process variables.² The engineering design of SSF systems has been hampered by the difficulty in making direct experimental measurements, which leads to a lack of mathematical models.

The aim of this work is to develop a mathematical model in order to evaluate the fundamental heat transfer mechanism in static SSF and more specifically to assess the importance of convection and conduction for heat dissipation. The experimental system selected was solid fermentation of cassava wet meal by *A. niger*. The conceptual basis of the model focuses on the growth characteristics of *A. niger*, a microorganism which has been extensively studied in SSF.^{6,8-11} The model consists of two parts: (a) a set of

simultaneous ordinary differential equations that describes the physiological processes, i.e., biomass growth, substrate consumption, and carbon dioxide production, as function of temperature, and (b) an energy balance which takes into account the accumulation, conduction, convection, and generation phenomena through dimensionless numbers. Further, one of the features of this model is to use the temperature records as the experimental basis to follow up the spatial and temporal distribution of microbial activity. It can predict carbon dioxide evolution which can be used as a continuous signal of microbial metabolism. Such a model should contribute to our understanding of heat transfer and generation mechanisms in SSF and could lead to improved design and control techniques in reactor systems.

MATERIALS AND METHODS

Microorganism

A strain of *Aspergillus niger*, var. *henebergii* (No. 10), described by Raimbault and Alazard² was used.

Inoculum

Spore suspension was prepared as described elsewhere.⁹ The inoculum size was 2×10^7 spores/g DM.

Pretreatment of Raw Material

Whole cassava (*Manihot esculenta*, var. *cubana*) meal was prepared using dry root chips obtained from Tabasco State, Mexico. Industrial grade mineral salts were added as follows (g/kg DM): ammonium phosphate 25 and ammonium sulfate 26. Salts were dissolved in tap water to a final moisture content of 38% adjusted to pH 3; the wet chips were gelatinized in a wet steam autoclave at 1 kg/cm^2 for 30 min. The mixture was then dried and milled at a mean particle size of 0.4–0.5 cm for its utilization.

Solid State Culture

The culture was realized under nonaseptic conditions as described previously⁸ but using a 1-L jacket glass bioreactor, 6 cm radius \times 35 cm long (Figs. 1a, 1b). In each trial 450 g of prepared cassava was humidified at 50%, inoculated, and packed at an apparent density of 0.75 kg/L ; the initial pH was 4.5. Incubation temperature was maintained at 35°C by recirculation of water through the jacket reactor and bubbling the inlet air in the water bath. The air flow was regulated at 0.2 L/h g DM , i.e., 90 h^{-1} in the whole reactor, the air section speed was 3500 cm/h .

Analysis

Carbon dioxide in the dry output air flow was monitored by an infrared Beckman analyzer, as described previously.^{6,10,11} Axial and radial temperature gradients in the fermenting mass were measured using a type J copper constantine ther-

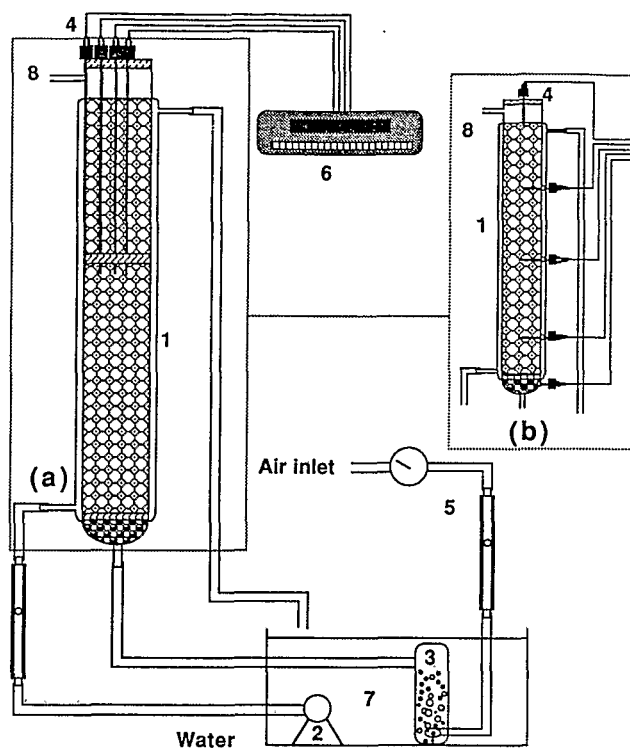


Figure 1. Experimental device for the monitoring of temperature gradient in solid fermentation of cassava by *A. niger*. (a) Radial gradient. (b) Axial gradient. Column fermentor; volume 1 L, 6 cm radius, 35 cm length: (1) jacket fermentor, (2) water pump, (3) humidifier, (4) thermocouples, (5) pressure and flow air controls, (6) temperature display device, (7) water bath.

mocouple, Eirelec, with a precision of 0.1°C . Temperature was measured at four positions along the radius at 0, 1.2, 2.4, and 3 cm. A fine double spiral acrylic grid plate was used to avoid interferences among thermocouples. Due to experimental limitations, either the radial or axial gradient was measured. Initial and final total true protein contents were measured by the Lowry method,¹² as applied earlier.¹⁰ Total biomass content was estimated on the basis of 47% of protein level previously measured on pure mycelium grown in submerged culture.⁶

MATHEMATICAL MODEL

Kinetic Model

A kinetic model for solid culture was proposed using as variables: biomass (X), sugar content (S), and carbon dioxide (CO_2), as applied earlier.^{6,13,14} It involves a logistic equation for the rate of microbial growth (R_x), and the rate of sugar consumption (R_s) proportional to the growth and maintenance energy (mX). Finally, the rate of carbon dioxide formation (R_g) is taken as a fraction of total sugar consumption. Logistic formulation stresses the concept that solid fermentation is a contact process limited by available surface area,^{6,15} with a maximal biomass packing density related with X_{max} and not included in conventional Monod model.¹⁶ It also assumes μ to be independent of substrate

concentration because the residual amount of sugar (around 30% DM) is considered to be much higher than the saturation constant (K_s) in Monod's equation; thus $\mu \approx \mu_{\max}$. A consequence of those assumptions is the independence of X_{\max} from substrate and CO_2 changes. The resulting set of ordinary differential equations is as follows:

$$R_x = \frac{dX}{dt} = \mu_{\max} X \left(1 - \frac{X}{X_{\max}} \right) \quad (1)$$

$$\text{at } t = 0 \quad X = X_0 \quad (1a)$$

$$R_s = \frac{-dS}{dt} = \frac{1}{Y_{X/S}} R_x + mX \quad (2)$$

$$\text{at } t = 0 \quad S = S_0 \quad (2a)$$

$$R_g = \frac{d\text{CO}_2}{dt} = Y_{\text{CO}_2} R_x \quad (3)$$

$$\text{at } t = 0 \quad \text{CO}_2 = 0 \quad (3a)$$

As a first approximation, the values of yield and maintenance coefficients were taken as reported by Raimbault⁶ and shown in Table II. Units of the variables are given in the nomenclature.

Temperature Dependence of Growth

From Equation (1), it can be seen that dependence of growth as a function of temperature can be described by the

Table I. Parameter estimation results of the heat transfer simulation in solid substrate fermentation of cassava by *Aspergillus niger*.

Run	m, E05	X_0 E04	Pe	Da_{III}	Bi	SS	MD (°C)
1	2.00	8.74	2551	8.61	10.12	82	0.14
2	2.86	4.40	2750	7.44	5.24	82	0.14

Note: SS: sum of Squares, $\Sigma(\text{Ti}_{\text{obs}} - \text{Ti}_{\text{cal}})^2$; MD: mean temperature deviation, $(\text{SS})^{1/2}/n$.

Table II. Values of the constants used in the simulation of heat transfer in SSF by *Aspergillus niger*.

Constant	Value	Units
u	3500	cm/h
μ_{\max}	0.3	1/h
X_{\max}	Eq. (5)	g % DM
dp	0.45	cm
F_{dm}	0.5	—
Φ	$8.57\text{E} - 03$	—
Ti	25	°C
S_0	75	g % DM
$Y_{X/S}$	0.55	g X/g S
Y_{CO_2}	0.29	g CO_2 /g S
L	30	cm
R_a	3	cm
R_{gi}	$1.85\text{E} - 06$	g % DM/h
ρ	0.7	g/cm ³
T_b	35	°C

specific growth constant (μ_{\max}) and the maximum biomass concentration (X_{\max}). Experimental μ_{\max} values were graphically estimated from four isothermal growth profiles using previous data.⁸ Due to the lack of experimental data, more "experimental" μ_{\max} data were interpolated by means of a polynomial fitting from 30 to 45°C. Data were then fitted to the expression proposed by Esener et al.¹⁷:

$$\mu_{\max} = \frac{A \exp(-E_{a1}/RT^*)}{1 + B \exp(-E_{a2}/RT^*)} \quad (4)$$

and parameters were estimated by the Marquardt algorithm,¹⁸ resulting in

$$A = 2.694\text{E} + 11 \text{ h}^{-1} \quad (4a)$$

$$B = 1.300\text{E} + 47 \quad (4b)$$

$$E_{a1} = 70,225 \text{ J/g mol} \quad (4c)$$

$$E_{a2} = 283,356 \text{ J/g mol} \quad (4d)$$

On the other hand, the X_{\max} profile as a function of temperature was approximated by a fourth order polynomial; the coefficients were as follows:

$$\begin{aligned} A_0 &= -127.08 & A_1 &= 7.95 & A_2 &= -0.016 \\ A_3 &= -4.03\text{E} - 03 & A_4 &= 4.73\text{E} - 05 \end{aligned} \quad (5)$$

Temperature profiles of μ_{\max} and X_{\max} are shown in Figure 2. In both cases a biphasic curve suggests an activation and inactivation process. Activation (E_{a1}) and inactivation (E_{a2}) energy values found in Equation (4) are in accordance with values found earlier.¹⁷

On the other hand, the effect of temperature on X_{\max} could be seen as affecting the fungal packing density (FPD). That is, Laukevics et al.¹⁵ have suggested that biomass concentration in SSF is correlated with FPD, which is maximal at optimal conditions. In other words, high fungal density could be self-limited, probably by diffusion limitations, depending on temperature.

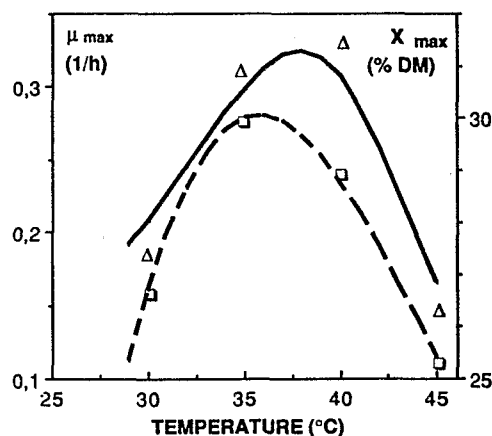


Figure 2. Comparison between experimental and calculated data for the dependence of μ_{\max} and X_{\max} as a function of temperature. Experimental μ_{\max} from Raimbault⁸ (Δ); calculated μ_{\max} by the Esener model¹⁷ [—, Eq. (4)]. Experimental X_{\max} from Raimbault⁸ (\square); calculated X_{\max} by a polynomial [---, Eq. (5)].

Since the experimental data were not complete, Equations (4) and (5) were used only as assumptions required for model development. The validity of this would be tested by looking at the agreement between observed and calculated data by the model.

Transport Model

The aim of this work was to develop a transport model in order to evaluate conduction and convection mechanisms in heat transfer of SSF. Assumptions were based on experimental and theoretical considerations.

Because of the low diffusion rate of biomass and glucose in solid media, the mass balance was not considered in this work. The heat accumulation was considered as the main limitation of microbial growth in SSF because the experimental evidence reported by Raimbault^{6,8} indicated strong growth inhibition for temperatures higher than 37°C (Fig. 2).

Considering the experimental difficulty in achieving accurate measurements in both solid and gas phases in SSF, a model which involves global coefficients on a pseudohomogeneous phase was preferred. According to the classification of Froment,¹⁹ a pseudohomogeneous model was selected over a heterogeneous one. Those kind of models have been largely used in packed bed chemical reactors.²⁰ Then, an energy balance in a cylindrical bioreactor was established using a pseudohomogeneous bidimensional dynamic model.^{19,21} Axial dispersion was not considered since the L/d_p ratio was around 80²⁰, and by neglecting variations in the Θ direction (i.e., assumption of symmetry), the equations are

$$\rho C_p \frac{\partial T'}{\partial t'} = k \left(\frac{\partial^2 T'}{\partial r'^2} + \frac{1}{r'} \frac{\partial T'}{\partial r'} \right) - u \rho C_p \frac{\partial T'}{\partial Z'} + \rho (-\Delta H) R_g \quad (6)$$

With the following boundary and initial conditions:

$$\text{BC at } r' = R_a \quad -k \frac{\partial T'}{\partial r'} = h(T' - T_b) \quad (6a)$$

and

$$\text{at } r' = 0 \quad \frac{\partial T'}{\partial r'} = 0 \quad (6b)$$

$$\text{IC at } t' = 0 \quad T' = T_i \quad (6c)$$

and

$$\text{at } Z' = 0 \quad T' = T_b \quad (6d)$$

Equations (6), (6a), (6b), (6c), and (6d) can be written in a dimensionless form²⁰ by using

$$r = \frac{r'}{R_a} \quad (7)$$

$$T = \frac{T'}{T_b} \quad (8)$$

$$Z = \frac{Z'}{L} \quad (9)$$

$$t = \frac{t'}{\Phi} \quad (10)$$

$$\Phi = \frac{L}{u} \quad (11)$$

The geometric reactor ratios L/R_a and R_a/d_p , the thermal diffusivity (α), and the dimensionless numbers Peclet (Pe), Biot (Bi), and Damköhler (Da_{III}) were introduced into the equations. The kinetic equations were expressed in dry matter basis. Then the dry mass fraction (F_{dm}) was considered in the heat generation term to simulate real fermentation conditions. Also the initial reaction rate value (R_{gi}) was used in the Damköhler number. The equations are

$$\frac{\partial T}{\partial t} = \frac{L d_p}{R_a^2 \text{Pe}} \left(\frac{\partial^2 T}{\partial r^2} + \frac{1}{r} \frac{\partial T}{\partial r} \right) - \frac{\partial T}{\partial Z} + F_{dm} Da_{III} \frac{1}{R_{gi}} R_g \quad (12)$$

The dimensionless boundary and initial conditions are

$$\text{BC at } r = 1 \quad -\frac{\partial T}{\partial r} = \text{Bi}(T - 1) \quad (12a)$$

and

$$\text{at } r = 0 \quad \frac{\partial T}{\partial r} = 0 \quad (12b)$$

$$\text{IC at } t = 0 \quad T = \frac{T_i}{T_b} \quad (12c)$$

and

$$\text{at } Z = 0 \quad T = 1 \quad (12d)$$

where

$$R_g = \frac{d\text{CO}_2}{dt} = Y_{\text{CO}_2} R_s \quad (13)$$

$$R_s = -\frac{dS}{dt} = \frac{1}{Y_{X/S}} R_s + mX\Phi \quad (14)$$

$$R_x = \frac{dX}{dt} = \mu_{m,x} X \left(1 - \frac{X}{X_{\max}} \right) \Phi \quad (15)$$

RESULTS AND DISCUSSION

Model Simplification

The verification of the whole model [Eqs. (12)–(15)] represents a difficult task in experimental and computational aspects. Thus a simplification based on experimental results was proposed.

Figure 3 shows the temperature evolution with time at different positions along the reactor axis and at the center of the column. It was noted that temperature profiles were not well defined as a function of the reactor length. Temperature data were plotted (Fig. 4) as a function of the reactor length at different fermentation times. It can be seen that from 5 to 35 cm the temperature gradient in the axial direction was small (0.17°C/cm). From 0 to 5 cm (Fig. 4), the reactor works as a heat exchanger rather than a fermenter.

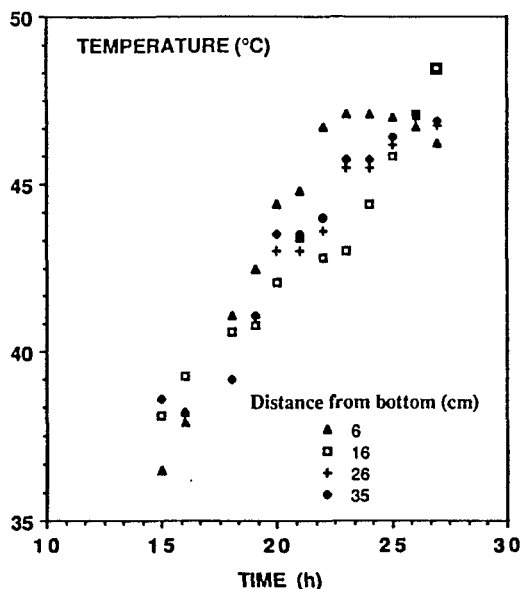


Figure 3. Evolution of the experimental temperature at different axis positions and at the center of the bioreactor.

tor. Thus for simulation studies the reactor length was considered to be 30 cm.

In similar experiments but monitoring the radial temperature gradient at 15 cm of the reactor top, a maximum difference of nearly 5°C/cm was found (Fig. 6) between the center and the wall of the reactor, that is, nearly 30 times greater than those compared with the axial gradient.

Reactor design and operating conditions can enhance the temperature gradient in one direction rather than the other. Rathbun and Shuler⁵ encouraged the gradients of temperature in the axial direction by using a reactor of cartesian geometry placed in a dry fan-type incubator and using a

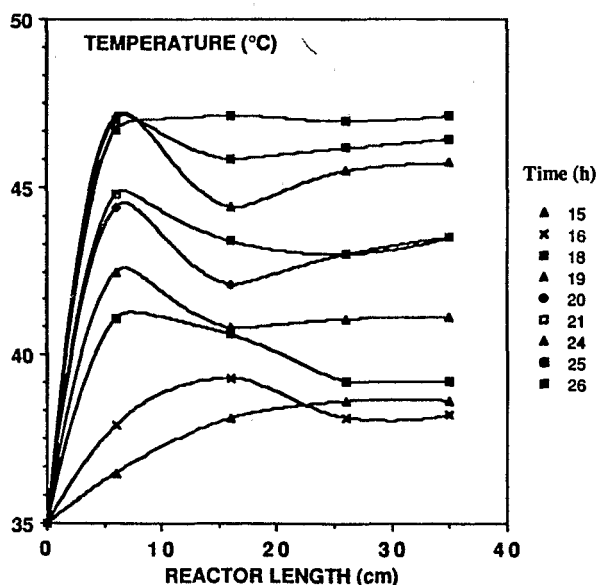


Figure 4. Variation of the experimental temperature as a function of the reactor length at different fermentation times.

high air flow rate. On the other hand, our reactor design and operating conditions enhanced the radial gradient of temperature rather than the axial one. These results are explained by the low air flow used, which also reduces the problems of air humidification and drying of fermenting mass. In other words, we have set conditions in such a way that the main heat transport resistance was conduction rather than convection.

Even when this simplification appears contradictory, the Peclet number remains in the model considering the ratio of convection and conduction heat transfer mechanisms in the packed bed bioreactor. The equation is

$$\frac{\partial T}{\partial t} = \frac{L d_p}{R_a^2 Pe} \left(\frac{\partial^2 T}{\partial r^2} + \frac{1}{r} \frac{\partial T}{\partial r} \right) + F_{dm} Da_{III} \frac{1}{R_{gi}} R_g \quad (16)$$

using the boundary and initial conditions defined by Equations (12a-c) and the reaction rate defined by Equations (13)-(15). It is called the simplified model.

Model Verification

Temperature is a function of radius and time simultaneously [Eq. (16)]. Model verification was realized by comparison of real and calculated temperature. Testing points were at 4 positions in the reactor radius during the fermentation time. A total of 64 experimental data points were used. Two independent fermentation data sets were used in parameter estimation. Temperatures were measured from 15 to 30 h of fermentation time, which is the period of most active mold growth. The spatial term on the right side of Equation (16) was discretized using the collocation orthogonal method.²² The resulting set of ordinary differential equations, from Equation (16), were integrated by a Runge-Kutta method.²³ Parameters were estimated through the Marquardt algorithm,¹⁸ which minimizes the sum of squares. In Figure 5 is

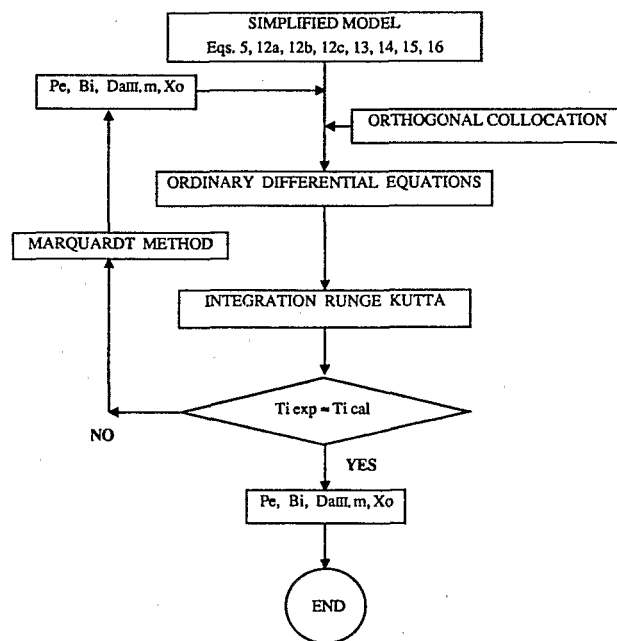


Figure 5. Program flow chart used for parameter estimation.

shown the program flow chart used for parameter estimation.

In order to verify this model, we carried out a number of regressions using a factorial-like design, considering μ_{\max} , X_{\max} , and the maintenance coefficient [Eq. (14)] in the estimation of Pe , Bi , and Da_{III} (Fig. 5). For example, μ_{\max} and X_{\max} could have assigned mean values of 0.3 h^{-1} and 30% DM, respectively or changes with temperature according to Equations (4) and (5), respectively. The maintenance coefficient could have values 0 and 0.07 or an estimated value provided by the algorithm in Figure 5. Constant μ_{\max} and X_{\max} in the same regression were not accepted since it does not simulate different growth profiles in the fermenting media.

Unsatisfactory results in regression analysis were obtained by using μ_{\max} defined by Equation (4), probably due to the sharp μ_{\max} variation beyond 37°C (Fig. 2). Best results as judged by the minimum sum of squares were obtained by holding μ_{\max} equal to 0.3, X_{\max} as function of temperature [Eq. (5)] and allowing an estimation of the coefficient of maintenance by the algorithm (Fig. 5). Estimates of initial biomass (X_0) were also found to be critical and were of the order of less than 1 mg/100 g DM.

Finally, the regressions were realized by changing inoculum size, maintenance energy, and Peclet, Biot, and Damköhler numbers in the simplified model [Eqs. (5), (12a)–(12c), and (13)–(16)]. Regression results are shown in Table I for two independent fermentation data sets. For both cases parameters values were in the same order of magnitude. Figures 6–8 correspond to run 1; the results for run 2 were very similar and are not shown. In Table II are shown the constant values used in the regressions.

As was expected, the main effect on calculated temperature profiles was in Pe , Bi , and Da_{III} estimations. Maintenance energy and inoculum size presented a lower effect in minimizing the sum of squares. Estimation of inoculum size, X_0 (Table I), were in good accordance with those values previously calculated by Raimbault⁶ (1.2×10^{-3}).

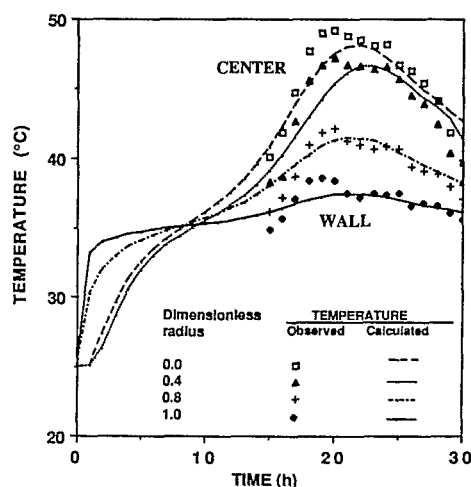


Figure 6. Comparison between calculated (—) and observed (symbols) temperature at different reactor radius during fermentation time.

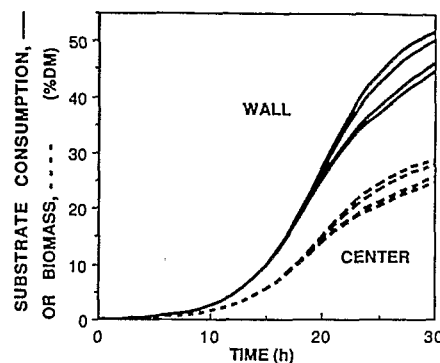


Figure 7. Evolution of the simulated biomass and sugar consumption at different reactor radius positions.

Nevertheless the calculated maintenance values were lower than those calculated by the same author (0.07).

Model verification was based on experimental and calculated temperature comparison. How well this worked is demonstrated in Figure 6, where the goodness of fit can be judged. Real data and predicted curves were in a good accordance since differences between calculated and observed values were very small (0.14°C). It suggests that the simplifications and principles used in model development and evaluation are correct.

The model simulates the biomass growth and sugar consumption (Fig. 7) inside the bioreactor. As expected, the biomass concentration and sugar consumption were more important near the wall than close to the reactor center. On the other hand, simulated final mean protein was 13.65% DM, considering 47% biomass content, which was in agreement with the experimental determination, 11.47% DM.

Further, carbon dioxide formation was simulated as a function of radius position, and a radial mean as a function

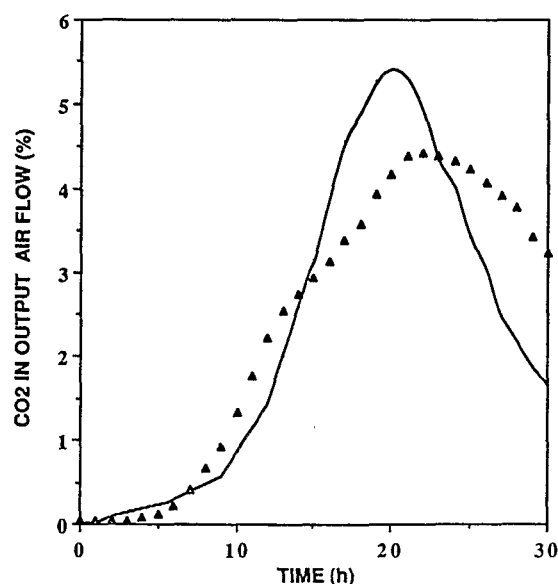


Figure 8. Comparison between calculated (—) and experimental (Δ) CO_2 .

of time was calculated. Even when CO_2 production was not a criterion for model testing, comparison of simulated and real gas production gives satisfactory results (Fig. 8).

The fermentation conditions lead to an estimation of 2550–2750 for the Peclet number and 5–10 for the Biot number in a laminar flow regime ($\text{Re}_{\text{dp}} = 1.61$). The Peclet and Biot estimations were high as compared with fixed bed chemical reactors, which can be explained by the organic nature of the material used, and the relatively low moisture starch limits the water content to 60% DM. The Biot number estimations indicate that the main heat transport resistance is found in conduction through the fixed fermentation bed rather than in the fermentor wall. On the other hand, Peclet number estimations indicate that the resistance of heat transfer by conduction is very high as compared with air convection.

This model contributes to our understanding of heat transport phenomena in SSF. We are proposing the use of dimensionless Peclet and Biot numbers as general criteria to evaluate various alternatives for temperature control of SSF, i.e., changing air flow rates and increasing water content. They could be used as scale-up criteria of large fermentors since those ratios describe the operation conditions, geometry, and size of the bioreactor. The model can be used also as a basis for reactor automatic control of SSF where a static fermentor is used. It can also be extended to other materials and microorganism systems where the product has a high added value.

The authors gratefully acknowledge the technical work of Ms. Luz Alarcon and Ms. Elisa Marquez and valuable suggestions of Dr. F. Lopez-Isunza, Dr. S. Revah, and Dr. N. G. Karanth. This work was carried out as a part of the cooperation agreement between the Consejo Nacional de Ciencia y Tecnología (CONACYT, Mexico) and the Institut Français de Recherche Scientifique pour le Développement en Coopération (ORSTOM, France), within a specific program research realized at the Universidad Autónoma Metropolitana (Mexico). The authors wish to thank the financial support of CONACYT, Organization of American States, and European Economic Community.

NOMENCLATURE

A	frequency factor (1/h)
A_i	polynomial coefficients
B	dimensionless factor in Arrhenius expression
Bi	dimensionless Biot wall number (hR_a/k)
CO_2	carbon dioxide (g CO_2 /100 g DM, g % DM)
C_p	thermal capacity (cal/g °C)
Da_{III}	dimensionless Damköhler number ($-\Delta H \rho L R_{gi}/u p C_p T_b$)
d_p	particle size (cm)
E_{a1}, E_{a2}	activation and inactivation energy (J/g mol K)
F_{dm}	fraction of dry matter
h	convective wall heat transfer coefficient
k	thermal conductivity (cal/cm h °C)
L	reactor length (cm)
m	energy maintenance constant (g X/g S h),
Pe	dimensionless Peclet heat number ($\alpha/d_p u$)
R	gas universal constant (J/g mol K)
R_a	reactor radius (cm)
Re_{dp}	dimensionless Reynolds particle number
R_g	carbon dioxide reaction rate (g % DM/h)
R_{gi}	initial carbon dioxide reaction rate at 35 °C
R_s	substrate consumption reaction rate (g % DM/h)

R_x	biomass reaction rate (g % DM/h)
r'	dimensional radius (cm)
S	consumed glucose (g/100 g DM, g % DM %)
T	dimensionless temperature (T'/T_b)
T'	dimensional temperature (°C)
T^*	absolute temperature (K)
T_i	initial temperature (°C)
T_b	incubation temperature (°C)
t'	time (h)
u	transversal velocity (cm/h)
X	biomass (g/100 g DM, g % DM)
X_{max}	maximum biomass concentration (g % DM)
X_0	initial biomass concentration
Y_{ds}	substrate to biomass yield (g X/g S)
Y_{CO_2}	substrate to carbon dioxide yield (g CO_2 /g S)
Z	dimensional axial direction (cm)

Greek symbols

α	thermal diffusivity ($k/\rho C_p$)
ΔH	reaction heat (cal/g S)
Φ	dimensional characteristic time (L/u)
μ_{max}	specific growth constant (1/h)
ρ	apparent density (g/cm ³)
Θ	angular direction

References

1. C. W. Hesseltine, *Biotechnol. Bioeng.*, **14**, 517 (1972).
2. M. A. Moo-Young, R. Moreira, and R. P. Tengerd, "Principles of Solid Substrate Fermentation," in *The Filamentous Fungi*, Vol. IV, S. E. Smith, D. R. Berry, and B. Vristiensen, Eds., (Arnold, London, 1983).
3. B. K. Lonsane, N. P. Ghildyal, S. Budiartman, and J. Ramakrishna, *J. Enz. Microb. Technol.*, **7**, 258 (1985).
4. S. M. Finger, R. T. Hatch, and T. M. Regan, *Biotechnol. Bioeng.*, **28**, 1193 (1976).
5. B. L. Rathbun and M. L. Shuler, *Biotechnol. Bioeng.*, **25**, 929 (1983).
6. M. Raimbault, *Fermentation in Milieu Solide*, ORSTOM, Trav. et Doc. No. 127, Paris (1981).
7. W. Grajek, *J. Ferment. Technol.*, **66**, 675 (1988).
8. M. Raimbault and D. Alazard, *Eur. J. Appl. Microbiol.*, **9**, 199 (1980).
9. M. Raimbault, S. Revah, F. Pina, and P. Villalobos, *J. Ferment. Technol.*, **63**, 395 (1985).
10. E. Oriol, M. Raimbault, S. Roussos, and G. Viniegra-Gonzalez, *Appl. Microbiol. Biotechnol.*, **27**, 498 (1988).
11. E. Oriol, B. Schettino, G. Viniegra-Gonzalez, and M. Raimbault, *J. Ferment. Technol.*, **66**, 57 (1987).
12. O. H. Lowry, N. J. Rosebrough, A. L. Farr, and R. J. Randal, *J. Biol. Chem.*, **193**, 265 (1951).
13. N. Okazaki, S. Sugama, and T. Tanaka, *J. Ferment. Technol.*, **58**, 471 (1980).
14. K. Sato and K. Yoshizama, *J. Ferment. Technol.*, **66**, 667 (1988).
15. J. J. Laukevics, A. F. Apsite, U. S. Viesturs, and R. P. Tengerd, *Biotechnol. Bioeng.*, **27**, 1687 (1985).
16. J. Monod, *Recherches sur la Croissance des Cultures Bactériennes* (Hermann, Paris, 1942).
17. A. A. Esener, J. A. Roels, and N. W. Kossen, *Biotechnol. Bioeng.*, **23**, 1401 (1981).
18. D. L. Marquardt, *J. Soc. Ind. Appl. Math.*, **11**, 431 (1963).
19. G. F. Froment, *Chem. Reaction Eng.*, Advances in Chem. Series No. 109 (American Chemical Society, Washington, DC, 1972).
20. J. Carberry, *Chemical and Catalytic Reaction Engineering*, (McGraw-Hill, New York, 1976).
21. H. Hlavacek, *Ind. Eng. Sci.*, **62**, 8 (1970).
22. B. A. Finlayson, *NonLinear Analysis in Chemical Engineering*, (McGraw-Hill, New York, 1980).
23. B. Carnahan, H. A. Luther, and J. O. Wilkes, *Applied Numerical Methods* (Wiley, New York, 1969).